Tanshinone IIA promotes osteogenic differentiation potential and suppresses adipogenic differentiation potential of bone marrow mesenchymal stem cells

WEI WANG[1*], HANGQIN WU[2*], SHUJING FENG[3*], XINGRUI HUANG[4], HAO XU[4], XINXIN SHEN[4], YAJING FU[5] and SHUCHEN FANG[4]

[1]Department of Orthopedics, Hubei Provincial Hospital of Traditional Chinese Medicine, Wuhan, Hubei 430074, P.R. China; [2]Department of Orthopedics, Wuyi County First People's Hospital, Wuyi, Zhejiang 321200, P.R. China; [3]School of Exercise and Health, Shanghai University of Sport, Shanghai 200438, P.R. China; [4]Department of Orthopedics, Suzhou Wujiang District Hospital of Traditional Chinese Medicine (Suzhou Wujiang District Second People's Hospital), Suzhou, Jiangsu 215003, P.R. China; [5]Department of Anesthesiology, Renmin Hospital of Wuhan University, Wuhan, Hubei 430072, P.R. China

Received May 20, 2024; Accepted July 18, 2024

DOI: 10.3892/mmr.2024.13301

Abstract. Tanshinone IIA (Tan IIA) may have therapeutic effects on avascular necrosis of the femoral head (ANFH) by targeting bone marrow mesenchymal stem cells (BMSCs). The effect and underlying mechanism of Tan IIA on adipogenesis and osteogenesis ability of BMSCs remain to be elucidated. In the present study BMSCs were treated with osteogenic or adipogenic differentiation medium with or without Tan IIA under hypoxic environment. Osteogenic differentiation potential was evaluated by alkaline phosphatase (ALP) measurement, alizarin red staining and reverse transcription-quantitative (RT-q) PCR of osteogenic marker genes. Adipogenic differentiation potential was evaluated with oil red staining and RT-qPCR of adipogenic marker genes. Detailed mechanism was explored by RNA-seq and small molecular treatment during osteogenesis and adipogenesis of BMSCs. ALP level, mineralized nodules and expression level of osteogenic marker genes significantly increased following Tan IIA treatment during osteogenic differentiation of BMSCs. Lipid droplet and expression levels of adipogenic marker genes significantly decreased following Tan IIA treatment during adipogenic differentiation of BMSCs. Gene Ontology and Kyoto Encyclopedia of Genes and Genomes analyses of RNA-seq data indicated increased Akt and TGFβ signaling following Tan IIA treatment. Further western blot assay confirmed that Tan IIA significantly activated Akt/cAMP response element-binding protein signaling and TGFβ/Smad3 signaling. Application of Akti1/2 (an Akt inhibitor) significantly decreased the promotion effect of osteogenesis induced by Tan IIA, while the addition of SB431542 significantly reduced inhibition effect of adipogenesis caused by Tan IIA. Tan IIA could promote osteogenic differentiation potential of BMSCs by activating AKT signaling and suppress adipogenic differentiation potential of BMSCs by activating TGFβ signaling.

Correspondence to: Dr Yajing Fu, Department of Anesthesiology, Renmin Hospital of Wuhan University, 238 Jiefang Road, Wuchang, Wuhan, Hubei 430072, P.R. China
E-mail: yajingfu1@qq.com

Dr Shuchen Fang, Department of Orthopedics, Suzhou Wujiang District Hospital of Traditional Chinese Medicine (Suzhou Wujiang District Second People's Hospital), 999 Dachun Road, Wujiang, Suzhou, Jiangsu 215003, P.R. China
E-mail: shuchenfang20@outlook.com

*Contributed equally

Key words: tanshinone IIA, bone marrow mesenchymal stem cells, avascular necrosis of the femoral head

Introduction

Avascular necrosis of the femoral head (ANFH) is a common orthopedic disease that is caused by disruption of blood supply near the proximal femur (1). It can bring severe pain, swelling, decreased leg strength and anesthesia (1). The majority of patients experience hip joint dysfunction in the development of disease for 1-4 years (2). There are several conservative and surgical methods to treat ANFH, including oral non-steroidal anti-inflammatory drugs, traditional Chinese medicine, physical therapy, lifestyle modification and even artificial hip replacement (3). However, there is still no consensus on the treatment of ANFH and the optimal treatment strategy should be further explored.

Bone marrow mesenchymal stem cells (BMSCs), a population of multipotent cells (4), play a crucial role in osteonecrosis repair by their osteogenic differentiation ability (5). The hypoxia environment in ANFH could significantly affect the physical function of BMSCs (6,7). Enhanced adipogenic differentiation ability and decreased osteogenic differentiation potential of BMSCs have been revealed in ANFH and the occurrence of ANFH is also closely associated with the changed differentiation direction of BMSCs (8). Thus, it is a promising strategy to treat ANFH by targeting BMSCs.

Salvia miltiorrhiza Bunge (also known as Danshen) is a popular traditional Chinese herbal medicine that exerts therapeutic effects on dilating blood vessels and ameliorating blood rheological properties (9). Therefore, it has been used to treat ANFH (10,11), although the in-depth mechanism behind how the active components function remains to be further investigated. Tanshinone IIA (Tan IIA) is one of the most abundant active compounds in *S. miltiorrhiza* and it is widely used to treat cerebrovascular and cardiovascular disease due to its antioxidant and anti-inflammatory ability (12). Furthermore, emerging studies indicate potential positive biological effects of Tan IIA for MSCs (13,14). It has been reported that Tan IIA can promote the *in vitro* migration of MSCs by increasing the expression of C-X-C chemokine receptor type 4 (CXCR-4) (13). Tan IIA also enhances expansion ability of BMSCs by regulating the progression of S phase of the cell cycle (14). In addition, Tan IIA can contribute to osteogenic differentiation of periodontal ligament stem cells (15) and mouse myoblast cell line C2C12 (16). Thus, Tan IIA might exert treatment potential for ANFH by targeting BMSCs. However, the role of Tan IIA in adipogenesis and osteogenesis of BMSCs remains to be elucidated.

Therefore, in the current study, the effect and underlying mechanism of Tan IIA on the adipogenesis and osteogenesis ability of BMSCs under hypoxic environment were explored. The findings will help illustrate the in-depth mechanism of how Tan IIA could treat ANFH by targeting BMSCs and thus providing solid experimental basis for ANFH treatment by using Tan IIA.

Materials and methods

Cell isolation, culture, differentiation and treatment. A total of 12 male C57BL/6 mice (age, 6 weeks; weight, ~16 gram) were obtained from the Animal Model Research Center of Nanjing University for BMSC isolation. The mice were housed under a 12-h light/dark cycle with *ad libitum* access to food and water, at a temperature of 20-26˚C and humidity of 40-60%. The BMSCs were isolated according to previous literature (17). Briefly, the mice were sacrificed and the muscles were dissected from the femurs. The femurs were cleaned by 1X phosphate buffer solution (PBS) and then fresh BMSCs were obtained by flushing the femoral cavity.

To mimic the hypoxic microenvironment in ANFH, the BMSCs were differentiated under hypoxic environment with 5% O_2c. The growth medium contains α-MEM (Gibco; Thermo Fisher Scientific, Inc.; cat. no. 12571071), 10% FBS (Gibco; Thermo Fisher Scientific, Inc.; cat. no. 10-013-CV) and 1% Penicillin-Streptomycin (Gibco; Thermo Fisher Scientific, Inc.; cat. no. 15140-122). The growth medium was replaced every three days. The BMSCs within three passages were used for osteogenic or adipogenic differentiation.

The growth medium was replaced by differentiated medium until BMSCs reached 90% confluence. Osteogenic medium (Procell Life Science & Technology Co., Ltd.; cat. no. PD-003-200) was used in osteogenic induction assays of BMSCs for 21 days. Adipogenic induction medium (AIM), containing high-glucose DMEM (Gibco; Thermo Fisher Scientific, Inc.; cat. no. 12100-046), 10% FBS, 1 μg/ml insulin (MilliporeSigma; cat. no. I2643), 0.25 μM dexamethasone (MilliporeSigma; cat. no. D4902), 0.5 mM 3-isobutyl-1-methylxanthine (MilliporeSigma; cat. no. I5879) and 1% penicillin-streptomycin, was applied in adipogenic differentiation assays for 14 days.

To explore the effect of Tan IIA, the BMSCs were induced by adipogenic and osteogenic differentiation medium with or without $5x10^{-5}$ mg/l Tan IIA.

In addition, 10 nM TGFβ signaling inhibitor SB431542 (Cell Signaling Technology, Inc.; cat. no. 14775S) (18) and 10 nM AKT signaling inhibitor Akti-1/2 (an Akt inhibitor; Tocris Bioscience; cat. no. 5773) (19) were applied to investigate the role of related signaling in BMSCs differentiation by being mixed with the differentiation medium. The differentiated assays were divided into three groups: DMSO, Tan IIA, Tan IIA + Akti 1/2 or SB431542.

Cell Counting Kit-8 assay. The Cell Counting Kit-8 (Beyotime Institute of Biotechnology; cat. no. C0038) kit was used according to the manufacturer's introductions. Briefly, the BMSCs were cultured with or without $5x10^{-5}$ mg/l Tan IIA for 24 h. The CCK8 solutions were added 20 μl/well. After 1 h, the absorbance at 450 nm was detected by a microplate reader (Thermo Fisher Scientific, Inc.).

Alkaline phosphatase assay. Alkaline Phosphatase Assay kit (Beyotime Institute of Biotechnology; cat. no. P0321S) was used to assess the osteogenic differentiation ability of BMSCs according to manufacturer's introductions. Briefly, the differentiated BMSCs were firstly lysed by western and IP lysis (Beyotime Institute of Biotechnology; cat. no. P0013) for 20 min. Then, the lysed product was incubated with chromogenic substrate at 37˚C for 15 min. Finally, the absorbance at 405 nm was measured by a microplate reader (Thermo Fisher Scientific, Inc.).

Alizarin red staining. At three weeks after osteogenic differentiation of BMSCs, BMSCs were fixed in 4% paraformaldehyde at room temperature for 20 min and then treated with Alizarin red (Beijing Solarbio Science & Technology Co., Ltd.; cat. no. G1452) at room temperature for 15 min. Then, the sample was washed three times by PBS and images captured under microscope. Cetylpyridinium chloride (10%) was used to dissolve the dye on the mineralized nodules. The absorbance values in each well at 490 nm were measured with a microplate reader and the images were captured by a light BX53 microscope (Olympus Corporation).

Oil red staining. Following adipogenic induction, BMSCs were fixed in 4% paraformaldehyde at room temperature for 20 min and treated with oil red (Beijing Solarbio Science & Technology Co., Ltd.; cat. no. G1260) at room temperature for 15 min. Then the sample was washed three times by 60% ethanol and images were captured under a light microscope. For lipid quantification analysis, the oil red was isolated with isopropanol for 5 min and the absorbance at 496 nm was measured by a microplate reader.

Gene expression analysis. BMSCs (90% confluence) were lysed for gene expression analysis. RNA extraction, cDNA synthesis and quantitative (q)PCR were performed according

Table I. Primer sequences of reverse transcription-quantitative PCR.

Gene	Sequence
Mouse Lpl Forward	5'-TTGCCCTAAGGACCCCTGAA-3'
Mouse Lpl Reverse	5'-TTGAAGTGGCAGTTAGACACAG-3'
Mouse Cebpa Forward	5'-GCGGGAACGCAACAACATC-3'
Mouse Cebpa Reverse	5'-GTCACTGGTCAACTCCAGCAC-3'
Mouse Perilipin 1 Forward	5'-CTGTGTGCAATGCCTATGAGA-3'
Mouse Perilipin 1 Reverse	5'-CTGGAGGGTATTGAAGAGCCG-3'
Mouse Gapdh Forward	5'-AGGTCGGTGTGAACGGATTTG-3'
Mouse Gapdh Reverse	5'-GGGGTCGTTGATGGCAACA-3'
Mouse Adipoq Forward	5'-GAAGCCGCTTATGTGTATCGC-3'
Mouse Adipoq Reverse	5'-GAATGGGTACATTGGGAACAGT-3'
Mouse Pparg Forward	5'-GGAAGACCACTCGCATTCCTT-3'
Mouse Pparg Reverse	5'-GTAATCAGCAACCATTGGGTCA-3'
Mouse Fabp4 Forward	5'-AAGGTGAAGAGCATCATAACCCT-3'
Mouse Fabp4 Reverse	5'-TCACGCCTTTCATAACACATTCC-3'
Mouse Bsp Forward	5'-TCCATCGAAGAATCAAAGCA-3'
Mouse Bsp Reverse	5'-AGTAGCGTGGCCGGTACTTA-3'
Mouse Ocn Forward	5'-AGACTCCGGCGCTACCTT-3'
Mouse Ocn Reverse	5'-CTCGTCACAAGCAGGGTTAAG-3'
Mouse Opn Forward	5'-GGAAACCAGCCAAGGTAAGC-3'
Mouse Opn Reverse	5'-TGCCAATCTCATGGTCGTAG-3'

to the manufacturers' protocols. Briefly, total RNA was obtained with EZ-press RNA Purification Kit (EZ Bioscience; cat. no. B0004DP). M-MuLV Reverse Transcriptase (New England BioLabs, Inc.; cat. no. M0253L) was used for reverse transcription (RT). The cDNA was synthesized at 42˚C for 1 h. To exclude contamination with genomic DNA, negative controls were set up during the reverse transcription step of the RNA to cDNA conversion. The cDNA was used for subsequent RT-qPCR with SYBR Green Master (Roche Diagnostics; cat. no. 4913914001) in a CFX96 System. The qPCR cycling conditions were as follows: 95˚C for 3 min; followed by 45 cycles at 95˚C for 5 sec and 60˚C for 30 sec; followed by an increase from 65 to 95˚C in increments of 0.5˚C for 5 sec, and maintenance at 4˚C. $2^{-\Delta\Delta Cq}$ was used to calculate the relative gene expressions. ΔΔCq indicates the differences between the difference of targets and control genes between control and treatment groups (20). The primers of RT-qPCR are listed in Table I.

Western blotting. Total proteins were obtained by western and IP lysis (Beyotime Institute of Biotechnology; cat. no. P0013) mixed with phenylmethylsulfonyl fluoride and Dithiothreitol. Protein concentration was measured using the BCA assay (Beyotime Institute of Biotechnology; cat. no. P0010S) according to the manufacturer's instructions. Total proteins (20 μg) in loading buffer were separated by SDS-PAGE on 10% gels and transferred to nitrocellulose membranes according to the standard methods (21). Full membranes were blocked with 5% BSA (Beyotime Institute of Biotechnology; cat. no. ST023) in TBST for 1 h at room temperature. Primary antibodies were incubated overnight at 4˚C: Anti-rabbit-GAPDH (Cell Signaling Technology, Inc.; cat. no. 2118L; 1:1,000), anti-rabbit-AKT (Cell Signaling Technology, Inc.; cat. no. 4865; 1:1,000), anti-rabbit-phosphorylated (p)-AKT (Cell Signaling Technology, Inc.; cat. no. 4060; 1:1,000), anti-rabbit-cAMP response element-binding protein (CREB; Proteintech Group, Inc.; cat. no. 12208-1AP; 1:1,000), anti-rabbit-phospho-CREB (Cell Signaling Technology, Inc.; cat. no. 9198S; 1:1,000), anti-rabbit-phospho-Smad3 (Absin Bioscience Inc.; cat. no. abs140144; 1:1,000), anti-mouse-Smad3 (Cell Signaling Technology, Inc.; cat. no. 9520; 1:1,000). Then the sample was incubated by HRP-conjugated secondary anti-rabbit or mouse antibodies (Santa Cruz Biotechnology, Inc.; cat. no. sc-2357; 1:3,000) for 1 h at room temperature. The target strips were obtained with ECL Reagent (ShareBio; cat. no. SBWB012).

Bulk RNA sequencing (RNA-Seq). Purified mRNA was first obtained (EZ Bioscience, cat. no. B0004DP) according to the instructions of manufacturer and RNA sequencing libraries were established by NEB Next Ultra RNA Library Prep Kit for Illumina (New England BioLabs, Inc.; cat. no. E7530L). Then, the cDNA library was established with non-stranded library preparation. Paired-end sequencing library was sequenced on the Illumina HiSeq xten sequencer (Illumina, Inc.) by 2x150 bp read length run. Gene abundances were quantified by RSEM (http://deweylab.biostat.wisc.edu/rsem/) (22). Differential expression analysis was performed using the DEGseq (23) and genes with P-value ≤0.001 were considered to indicate a statistically significant difference. Kyoto Encyclopedia of Genes and Genomes (KEGG) and Gene Ontology (GO) analysis were carried out by KOBAS (http://kobas.cbi.pku.edu.cn/home.do) and Goatools (https://github.com/tanghaibao/Goatools) (24). RNA sequencing data has been uploaded to NCBI (https://www.ncbi.nlm.nih.gov/; accession no.: PRJNA1131477).

Animals. Animal experiments were approved by the animal ethics committee of Suzhou Wujiang District Second People's Hospital (approval no. WZY2022056; Suzhou, China). A total of 10 wild-type female mice (age, 8 weeks; weight, ~18 g) were procured from Shanghai Jihui Laboratory Animal Care Co., Ltd. for subsequent experiments. The mice were housed as aforementioned. Their health status was monitored weekly. Tri-bromoethanol (250 mg/kg) was used as an anesthetic to minimize discomfort. Following the establishment of an ovariectomy model in mice, tan IIA was administered to explore its osteogenic potential *in vivo*. Over a period of four weeks, intraperitoneal injections were administered every other day. At the end of an eight-week period post-surgery, mice were sacrificed with CO_2, confirmed by the cessation of breathing and heartbeat for at least five minutes.

Micro-computed tomography (CT) analysis. Femurs were collected and fixed in 4% paraformaldehyde at room temperature for 24 h. The samples were then washed with PBS before being subjected to micro-CT scanning (Bruker micro-CT; Bruker Corporation). The micro-CT data were analyzed to assess bone morphology and density.

Statistical analysis. Statistical analysis was conducted by SPSS version 19.0 for Windows (IBM Corp.). Unpaired Student's t-test was used to compare two groups of experimental data, whereas one-way analysis of variance and Tukey test were used to compare quantitative parameters between more than two groups. All the experiment results were presented as mean ± standard deviation. Each experiment was repeated three times. All assays were blindly assessed and analyzed by two independent investigators. $P<0.05$ was considered to indicate a statistically significant difference.

Results

Tan IIA promotes osteogenic differentiation of BMSCs. The CCK-8 assay was used to measure the toxicity of Tan IIA and determine the concentration of Tan IIA in the current study (Fig. 1). Finally, the $5x10^{-5}$ mg/l Tan IIA was used in subsequent experiments. To evaluate the effects of Tan IIA on osteogenic differentiation of BMSCs, the BMSCs were cultured in osteogenic induction medium with or without Tan IIA. At seven days following osteogenic induction of BMSCs, Tan IIA significantly increased alkaline phosphatase (ALP) level when compared with control (Fig. 2A and B). The Alizarin red staining revealed that Tan IIA significantly enhanced mineralized nodules after 21 days of osteogenic differentiation (Fig. 2C). RT-qPCR results also found increased expression of osteogenesis marker genes, including osteocalcin (Ocn), bone sialoprotein (Bsp) and osteopontin (Opn) and following treatment of Tan IIA (Fig. 2D). Taken together, these results demonstrated that Tan IIA promoted osteogenic differentiation of BMSCs.

Tan IIA suppresses adipogenic differentiation of BMSCs. To evaluate the effects of Tan IIA on adipogenic differentiation of BMSCs, the BMSCs were cultured in adipogenic induction medium with or without Tan IIA for subsequent assays. At 10 days after adipogenic induction of BMSCs, oil red staining revealed that Tan IIA significantly suppressed

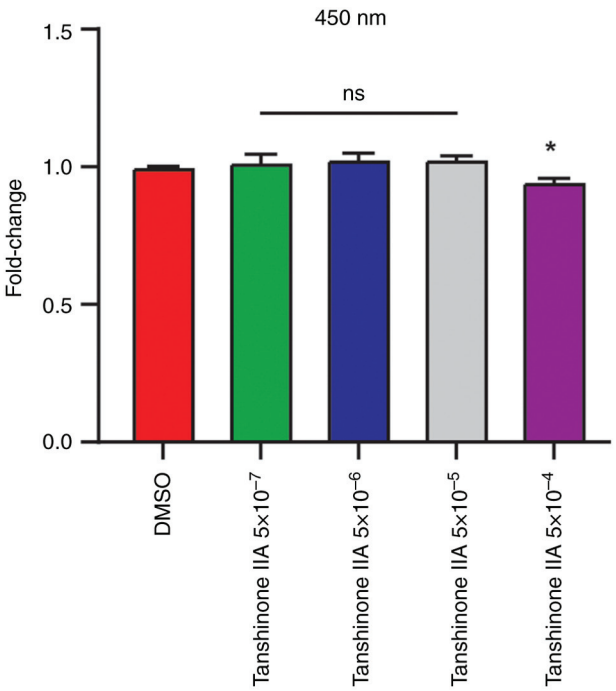

Figure 1. CCK-8 assay was used to explore the concentration of Tan IIA (mg/l) during treatment of BMSCs. ns, not significant. *P<0.05. Tan IIA, Tanshinone IIA; BMSCs, bone marrow mesenchymal stem cells.

formation of lipid droplets when compared with control (Fig. 3A and B). Furthermore, RT-qPCR results also found decreased expression of adipogenic marker genes, including perilipin1 (Plin1), fatty acid-binding protein (Fabp4), adiponectin (Adipoq), CCAAT/enhancer binding protein alpha (Cebpa), peroxisome proliferators-activated receptors gamma (Pparg) and lipoprteinlipase (Lpl) following treatment of Tan IIA (Fig. 3C). Taken together, these results demonstrated that Tan IIA suppressed the adipogenic differentiation of BMSCs.

RNA-seq reveals activated TGFβ and AKT signaling of BMSCs following Tan IIA treatment. The present study next performed RNA-sequence to compare the expression profile between BMSCs with or without Tan IIA treatment. The differentially expressed gene analysis revealed there were 1,477 upregulated genes and 1932 down-regulated genes following treatment of Tan IIA (Fig. 4A and B). The GO analysis of upregulated genes enriched key terms, including osteoblast differentiation, regulation of ossification and bone morphogenesis (Fig. 4C), which was consistent with aforementioned phenotype that Tan IIA could promote osteogenic differentiation of BMSCs. In addition, the GO analysis of downregulated genes enriched key terms, including lipid catabolic process, fatty acid metabolic process and fat cell differentiation (Fig. 4C), which was also consistent with the results that Tan IIA could inhibit adipogenic differentiation of BMSCs.

To further investigate the potential mechanism of how Tan IIA affected differentiation potential of BMSCs, KEGG analysis of upregulated genes was performed and TGFβ signaling pathway, AKT signaling pathway and cAMP signaling pathway were enriched (Fig. 4D). SMAD protein signaling transduction was also enriched in GO analysis of upregulated genes

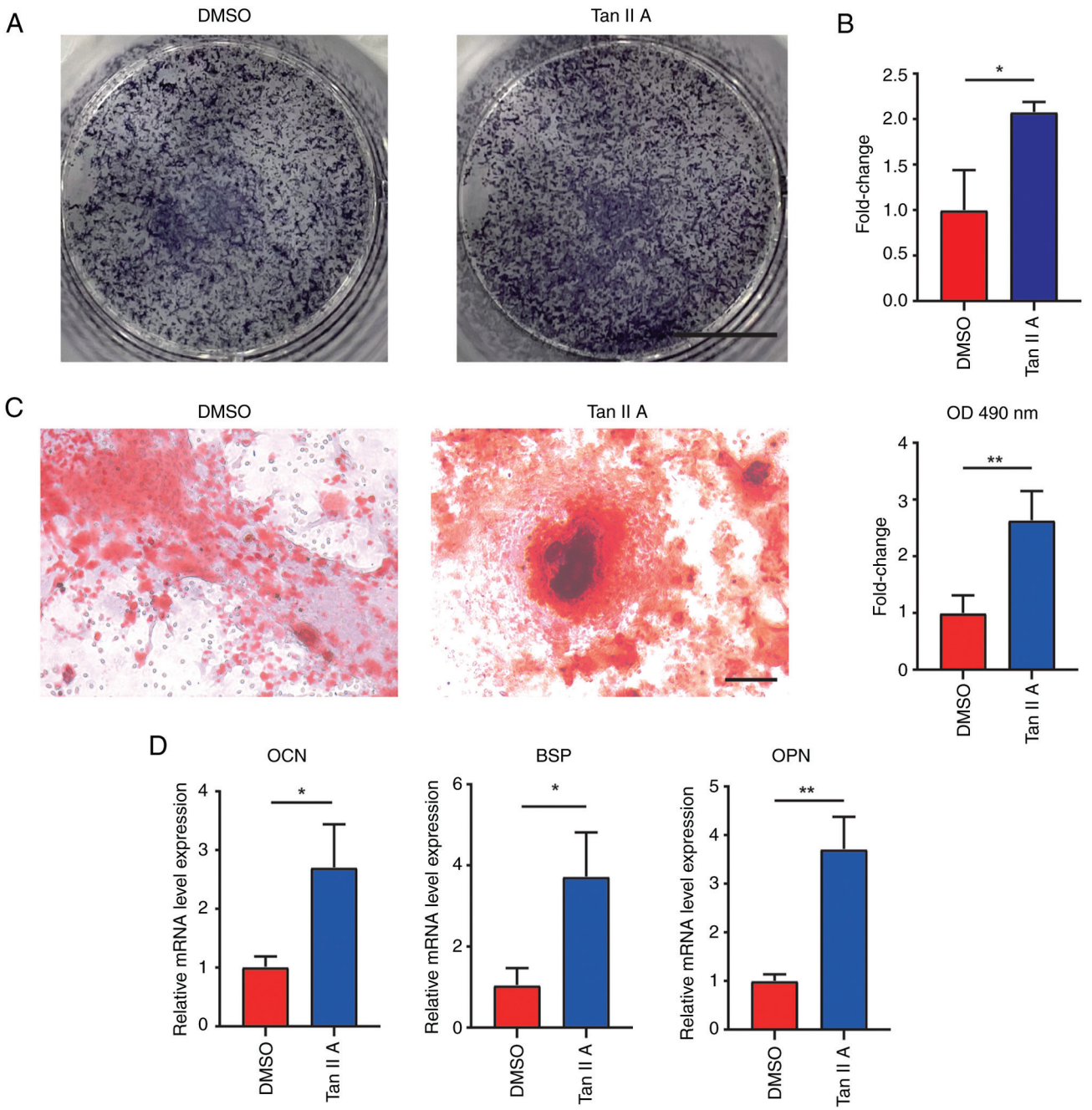

Figure 2. Tan IIA promotes osteogenic differentiation of BMSCs. (A) ALP staining for BMSCs and (B) measurement of ALP in BMSCs following osteogenic differentiation for 7 days with or without Tan IIA treatments. Scale bar, 5 mm. (C) Alizarin red staining of BMSCs following osteogenic differentiation for 21 days in DMSO and Tan IIA groups. Scale bar, 100 μm. (D) Gene expression of Ocn, Bsp and Opn in BMSCs following osteogenic differentiation for 21 days in DMSO and Tan IIA groups. *P<0.05, **P<0.01. Tan IIA, Tanshinone IIA; BMSCs, bone marrow mesenchymal stem cells; ALP, alkaline phosphatase; Ocn, osteocalcin; Bsp, bonesialoprotein; Opn, osteopontin.

(Fig. 4C). Smad3 is a downstream effector of TGFβ signaling and plays a crucial role in inhibiting adipogenesis (25-27).

Western blot assay also demonstrated that TGFβ/Smad3 signaling was activated following Tan IIA treatment (Fig. 5A and C). It is known that CREB is the classic effector in cAMP and AKT/CREB signaling significantly contributes to osteogenesis (28-31). Western blotting also demonstrated that AKT/CREB signaling was significantly activated following Tan IIA treatment (Fig. 5B and C). Taken together, these data revealed activated TGFβ and AKT signaling pathways following Tan IIA treatment.

Tan IIA promoted osteogenic differentiation of BMSCs through AKT signaling. Next, the present study explored whether Tan IIA promoted osteogenic differentiation of BMSCs through activating AKT signaling. Akti 1/2 is a known AKT signaling inhibitor and it was added in the presence of Tan IIA during the osteogenic differentiation of BMSCs. At seven days following osteogenic induction, the group containing both Akti 1/2 and Tan IIA contributed to decreased ALP levels when compared with Tan IIA group (Fig. 6A and B). Alizarin red staining revealed that Akti 1/2 significantly reduced mineralized nodules after 21 days of

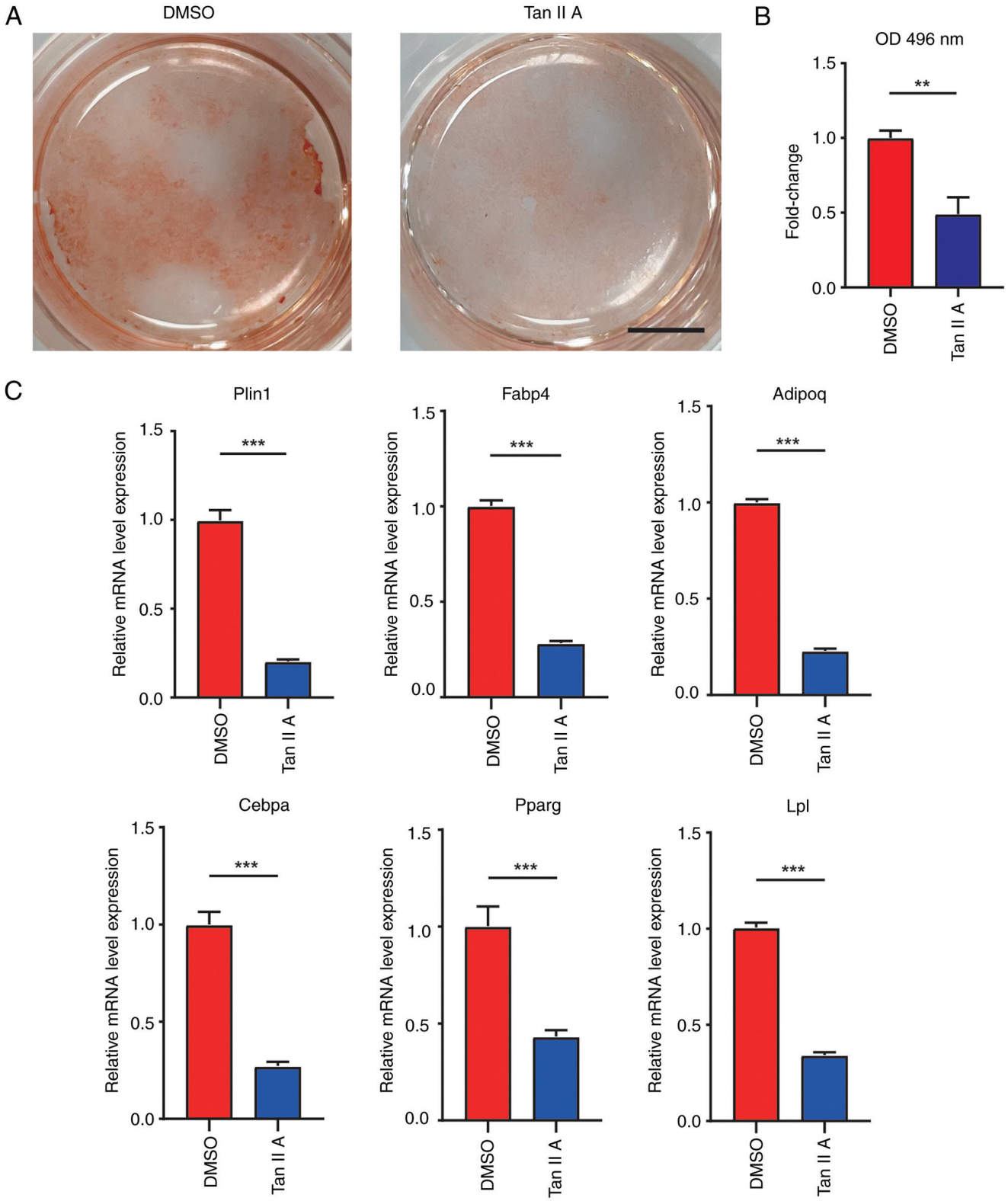

Figure 3. Tan IIA suppresses adipogenic differentiation of BMSCs. (A) Oil red staining of BMSCs following adipogenic differentiation for 14 days in DMSO and Tan IIA groups. Scale bar, 5 mm. (B) Quantification analysis of oil red staining in DMSO and Tan IIA groups. (C) Gene expression of Plin1, Fabp4, Adipoq, Cebpa, Pparg and Lpl of BMSCs following adipogenic differentiation for 14 days in control and Tan IIA groups. **P<0.01, ***P<0.001. Tan IIA, Tanshinone IIA; BMSCs, bone marrow mesenchymal stem cells; Plin1, perilipin1; Fabp4, fatty acid-binding protein; Adipoq, adiponectin; Cebpa, CCAAT/enhancer binding protein alpha; Pparg, peroxisome proliferators-activated receptors gamma; Lpl, lipoprteinlipase.

osteogenic differentiation (Fig. 6C). Furthermore, RT-qPCR results also found decreased expression of osteogenic marker genes, including Ocn, Opn and Bsp following addition of Akti 1/2 (Fig. 6D). Taken together, these results demonstrated that Tan IIA promoted osteogenic differentiation of BMSCs by activating AKT signaling pathway.

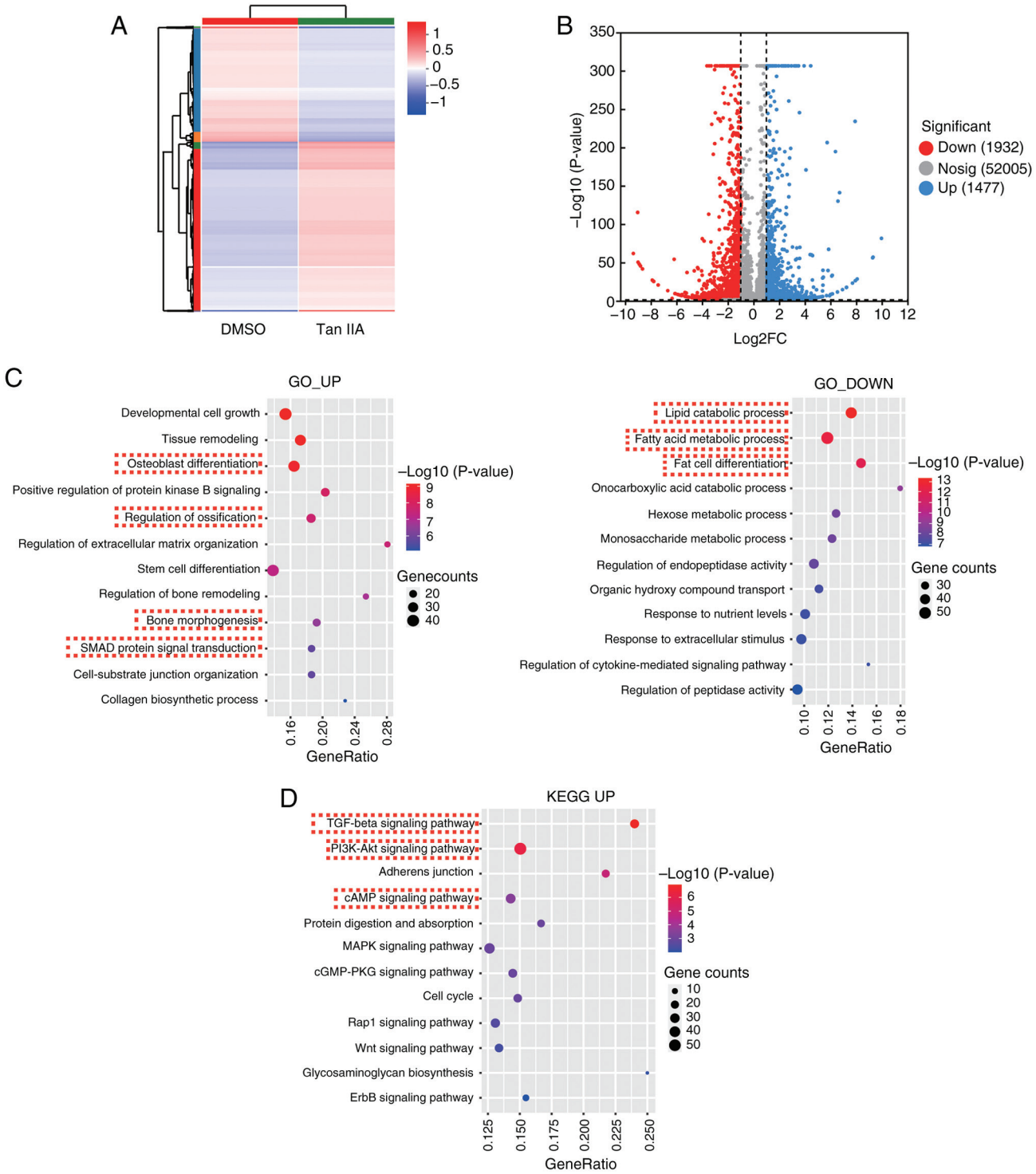

Figure 4. RNA-seq reveals activated TGFβ and Akt signaling of BMSCs following Tan IIA treatment. (A) Heatmap of clustering analysis for differentially expressed genes of BMSCs between control and Tan IIA group. (B) Volcano map for differentially expressed genes of BMSCs between control and Tan IIA group. (C) GO analysis of upregulated and downregulated genes of BMSCs in Tan IIA group. (D) KEGG analysis of upregulated genes of BMSCs in Tan IIA group. Tan IIA, Tanshinone IIA; BMSCs, bone marrow mesenchymal stem cells; GO, Gene Ontology; KEGG, Kyoto Encyclopedia of Genes and Genomes.

Tan IIA suppresses the adipogenic differentiation of BMSCs through TGFβ signaling. The present study also explored whether Tan IIA suppressed adipogenic differentiation of BMSCs through activating TGFβ signaling. SB431542 is a known TGFβ signaling inhibitor and it was added in the presence of Tan IIA during adipogenic differentiation of BMSCs. At 10 days after adipogenic induction of BMSCs, oil red staining revealed that the group containing both Tan IIA and SB431542 significantly increased formation of lipid droplets when compared with Tan IIA group (Fig. 7A and B). Furthermore, RT-qPCR results also found increased expression of adipogenic marker genes including Adipoq, Cebpa, Pparg, Fabp4, Lpl and Plin1 following inhibition of TGFβ signaling (Fig. 7C). Although the Fabp4 and Lpl levels did

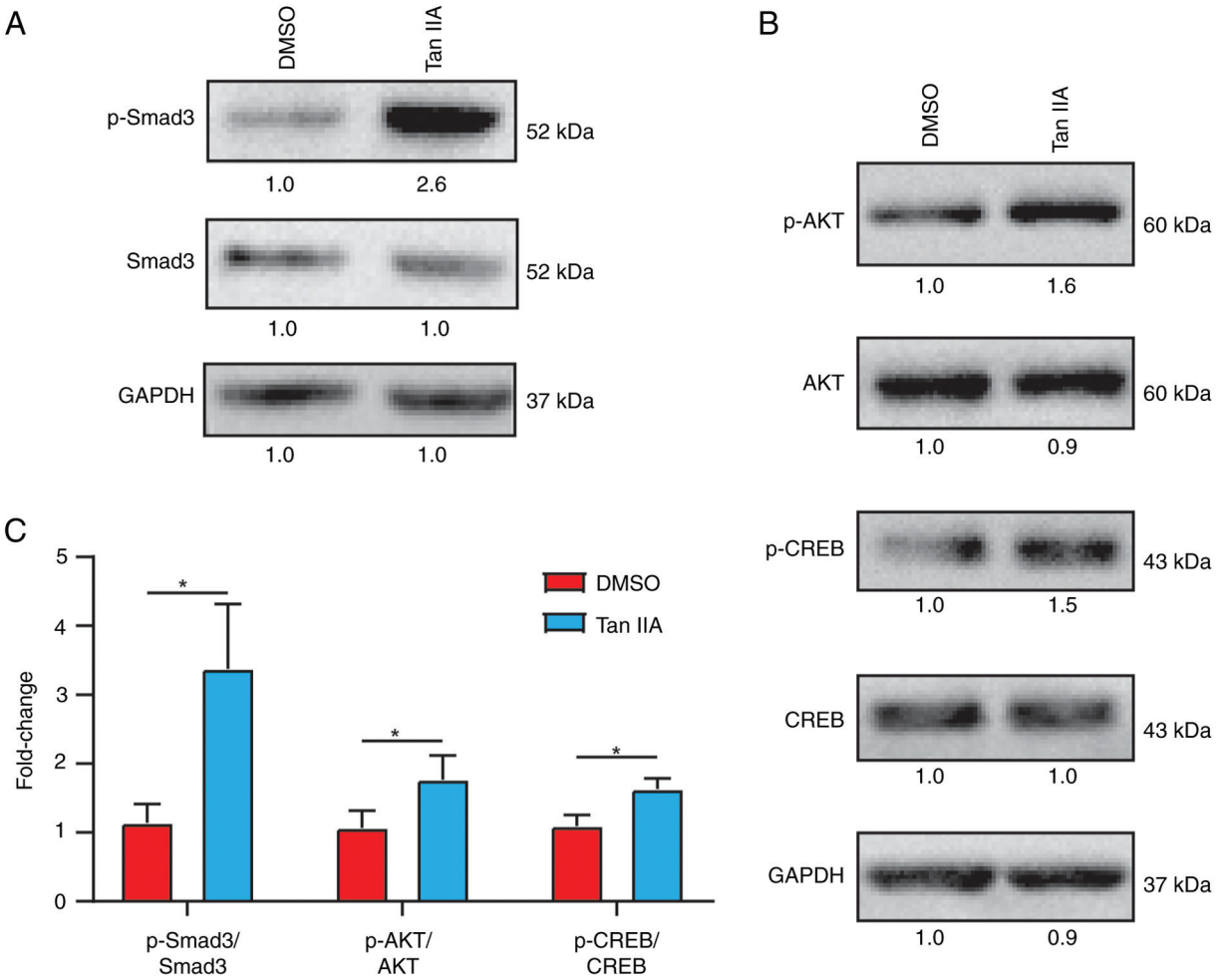

Figure 5. Western blotting demonstrates activated TGFβ and Akt signaling of BMSCs following Tan IIA treatment. (A) Protein level of p-Smad3, Smad3 and GAPDH and (B) p-Akt, Akt, p-CREB, CREB and GAPDH of BMSCs in DMSO and Tan IIA group. (C) Quantity analysis of western blots. *P<0.05. BMSCs, bone marrow mesenchymal stem cells; Tan IIA, Tanshinone IIA; p-, phosphorylated; CREB, cAMP response element-binding protein.

not reach statistical significance (Fig. 7C). Taken together, these results demonstrated Tan IIA suppressed the adipogenic differentiation of BMSCs by activating TGFβ signaling pathway.

Tan IIA Promotes BMSCs osteogenesis in vivo. To further investigate the osteogenic potential of Tan IIA *in vivo*, an ovariectomy model was established in mice and treated with Tan IIA. Micro-CT analysis revealed that Tan IIA inhibited bone loss in the ovariectomy models (Fig. 8A-D), indicating its pro-osteogenic potential for BMSCs *in vivo*.

Discussion

ANFH is caused by the interruption of blood supply to the femoral head, leading to necrosis of localized tissue, which further affects the femoral head located in the hip joint (1). BMSCs are multipotent stem cells with the potential for self-renewal and multidirectional differentiation (adipogenesis, osteogenesis and chondrogenesis) (4).

In the case of osteonecrosis, BMSCs can migrate and undergo directional differentiation into osteoblasts, actively participating in the bone repair process (8). However, BMSCs show unsatisfactory functions in ANFH. There are two main reasons: One is that limited blood supply of femoral head makes it difficult for MSCs to reach the necrotic area. Another is that insufficient blood supply leads to a decreased oxygen level, which can downregulate the expression of key osteogenic genes [such as BMP-2 and runt-related transcription factor 2 (RUNX2)], thereby inhibiting the ability of MSCs to differentiate into osteoblasts (4). Thus, there is decreased osteogenesis potential and increased adipogenesis ability for BMSCs from ANFH (8). Effective strategy is required to treat ANFH by correcting the differentiation direction of BMSCs.

It has been reported that *Salvia miltiorrhiza* Bunge could promote the osteogenesis and inhibit bone resorption and thus it exerts favorable preventive effects on bone loss (32). Emerging studies have shown that some Chinese herbal formulas containing *S. miltiorrhiza*, including Gufang Xian, Ling Gu Bao and Huo-gu are effective in treating ANFH (33,34). In addition, *S. miltiorrhiza* could also promote the migration of MSCs and contribute to the re-ossification and revascularization of ANFH in rabbit model of ANFH (11). However, the underlying pharmacological mechanisms of which active component and how it functions were unknown before the current study, to the best of the authors' knowledge.

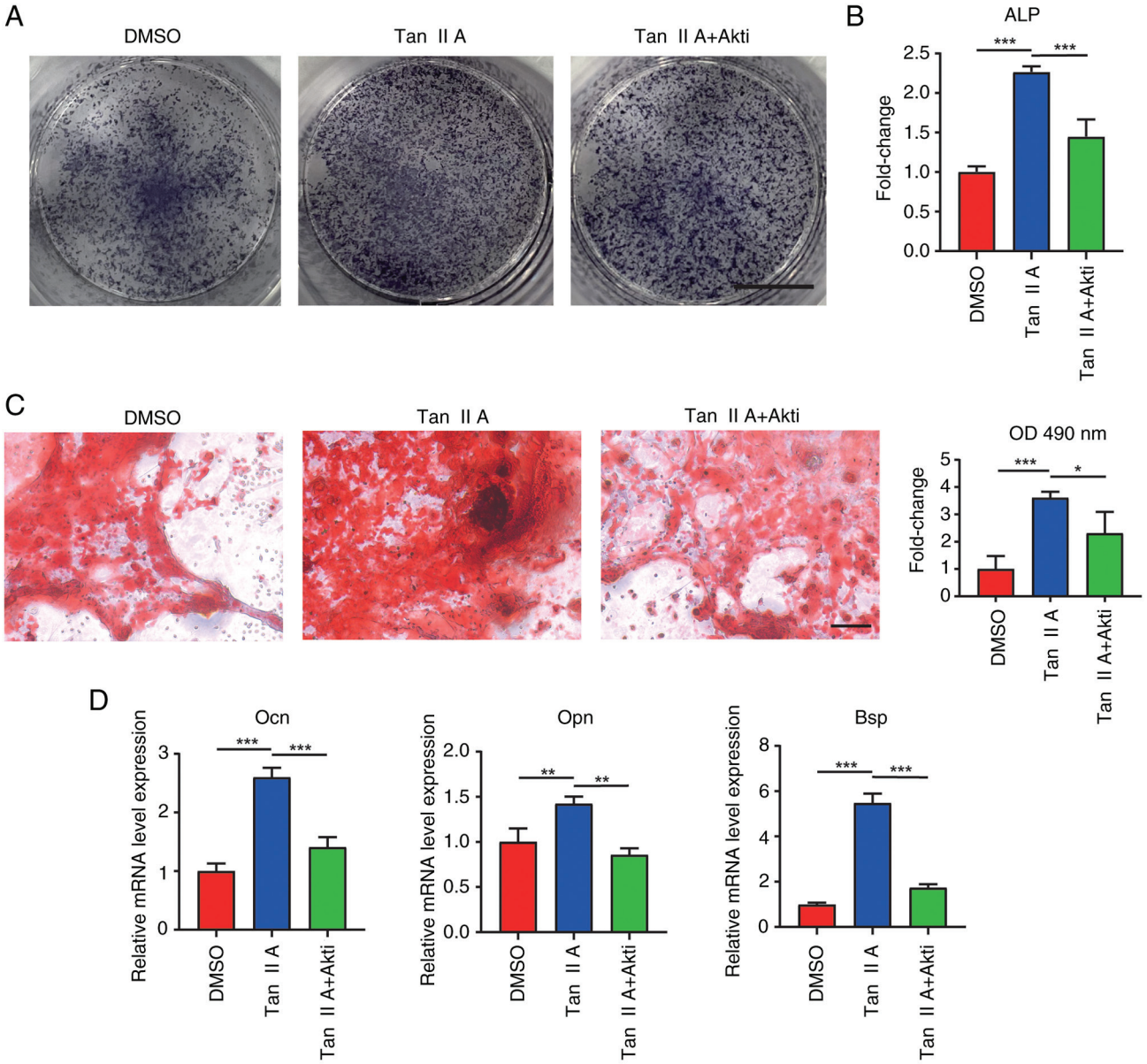

Figure 6. Tan IIA promotes osteogenic differentiation of BMSCs through Akt signaling. ALP staining for BMSCs following osteogenic differentiation for 7 days. The freshly isolated BMSCs were differentiated in an osteogenic induction medium (DMSO group) or with Tan IIA treatment (Tan IIA group) or Tan IIA supplemented with Akt signaling inhibitor Akti 1/2 treatment (Tan IIA + Akti 1/2 group). (A and B) Measurement of ALP in BMSCs following osteogenic differentiation for 7 days. Scale bar, 5 mm. (C) Alizarin red staining of BMSCs following osteogenic differentiation for 21 days with different treatments, Scale bar, 100 μm, and quantification analysis of mineralized nodules of BMSCs following osteogenic differentiation for 21 days with different treatments. (D) Gene expression of Ocn, Opn and Bsp in BMSC following osteogenic differentiation for 21 days with different treatments. *P<0.05, **P<0.01, ***P<0.001. BMSCs, bone marrow mesenchymal stem cells; Tan IIA, Tanshinone IIA; Ocn, osteocalcin; Bsp, bonesialoprotein; Opn, osteopontin.

As one of the most abundant active lipophilic compounds in *S. miltiorrhiza*, previous studies have indicated potential positive biological effects of Tan IIA for MSCs. MSCs treated with Tan IIA show increased CXCR4 and thus obtain enhanced migration ability (13). In addition, Tan IIA also increases the *ex vivo* expansion of human BMSCs by fibroblast growth factor 2-mediated PI3K/AKT signaling pathways (14). Furthermore, there are studies indicating the function of Tan IIA in osteogenesis (15,16,35). Li *et al* (35) demonstrate that Tan IIA can block the apoptosis of osteoblasts induced by dexamethasone via inhibiting Nox4-derived ROS production. Korean researchers found that Tan IIA can promote the osteogenic differentiation of mouse muscle cell line C2C12 cells with BMP2 (16). This effect was achieved by enhancing the activity of P38, which further promoted the activity of Runx2 (16). Liu *et al* (15) demonstrate that Tan IIA can also contribute to osteogenesis of human periodontal ligament stem cells via ERK1/2-dependent Runx2 induction. The current study revealed enhanced osteogenic differentiation ability and decreased adipogenic differentiation ability of BMSCs following treatment of Tan IIA. To the best of the authors' knowledge, it is the first time that effects of Tan IIA for osteogenesis and adipogenesis of BMSCs under hypoxia environment were investigated. Thus, the current study provided a promising application prospect for Tan IIA to treat ANFH by targeting BMSCs.

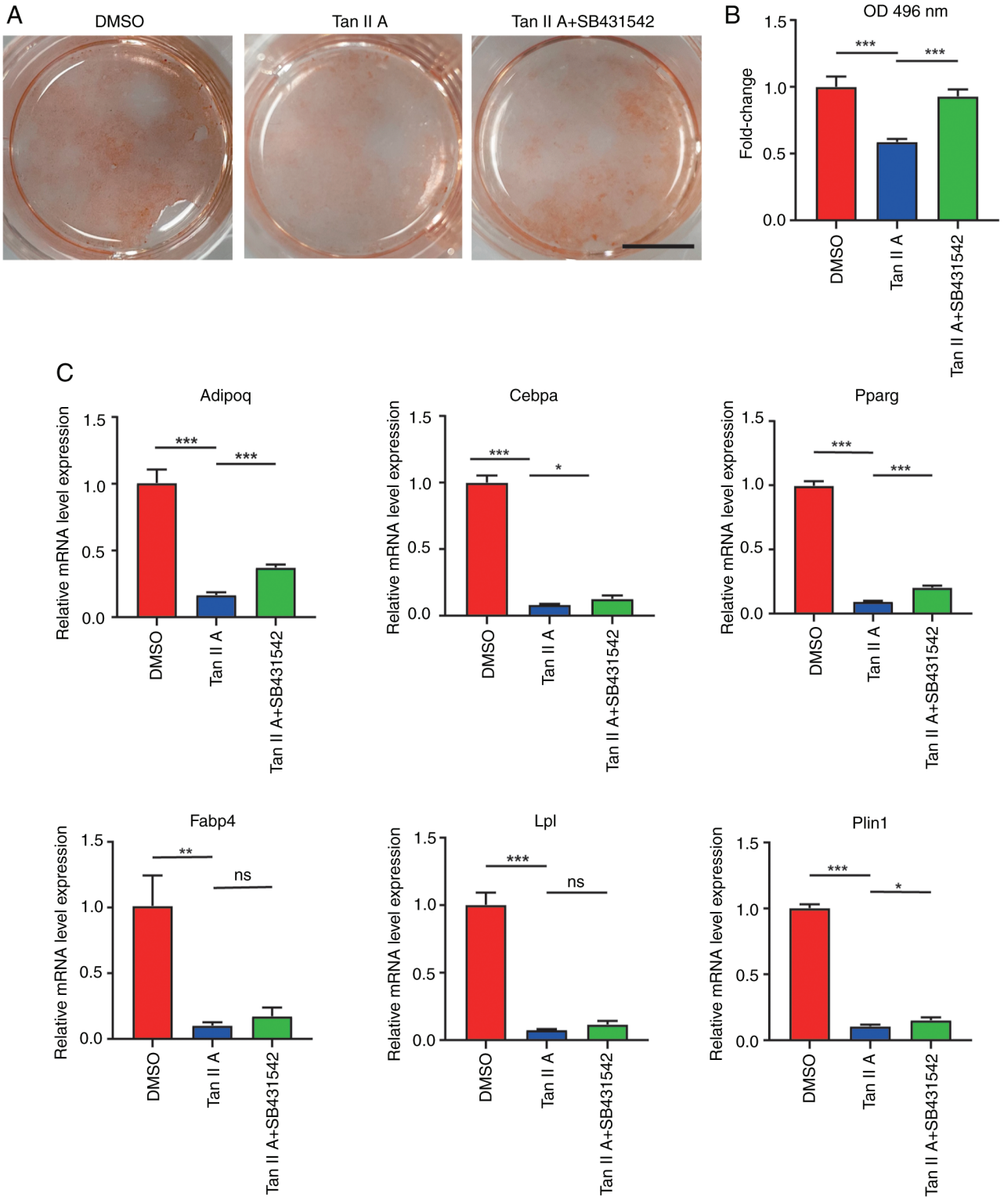

Figure 7. Tan IIA suppresses the adipogenic differentiation of BMSCs through TGFβ signaling. (A) Oil red staining of BMSCs following adipogenic differentiation for 14 days. The freshly isolated BMSCs was differentiated in an adipogenic induction medium (DMSO group) or with Tan IIA treatment (Tan IIA group) or Tan IIA supplemented with TGFβ signaling inhibitor SB431542 treatment (Tan IIA + SB431542 group). Scale bar, 5 mm. (B) Quantification analysis of oil red staining of BMSCs following adipogenic differentiation for 14 days with different treatments. (C) Gene expression of Plin1, Pparg, Cebpa, Fabp4, Adipoq and Lpl in BMSC following adipogenic differentiation for 14 days with different treatments. *P<0.05, **P<0.01, ***P<0.001, ns P>0.05. Tan IIA, Tanshinone IIA; BMSCs, bone marrow mesenchymal stem cells; Plin1, perilipin1; Fabp4, fatty acid-binding protein; Adipoq, adiponectin; Cebpa, CCAAT/enhancer binding protein alpha; Pparg, peroxisome proliferators-activated receptors gamma; Lpl, lipoprteinlipase.

The transcription factor CREB is a regulatory target for AKT (36) and the role of AKT/CREB signaling in osteogenesis has been solidly demonstrated (28-31). Cao *et al* (28) found that the osteogenic potency of MSCs can be maintained by activating AKT/CREB pathway in the presence of steroids. Kang *et al* (29) illustrate that phosphorylated AKT can react

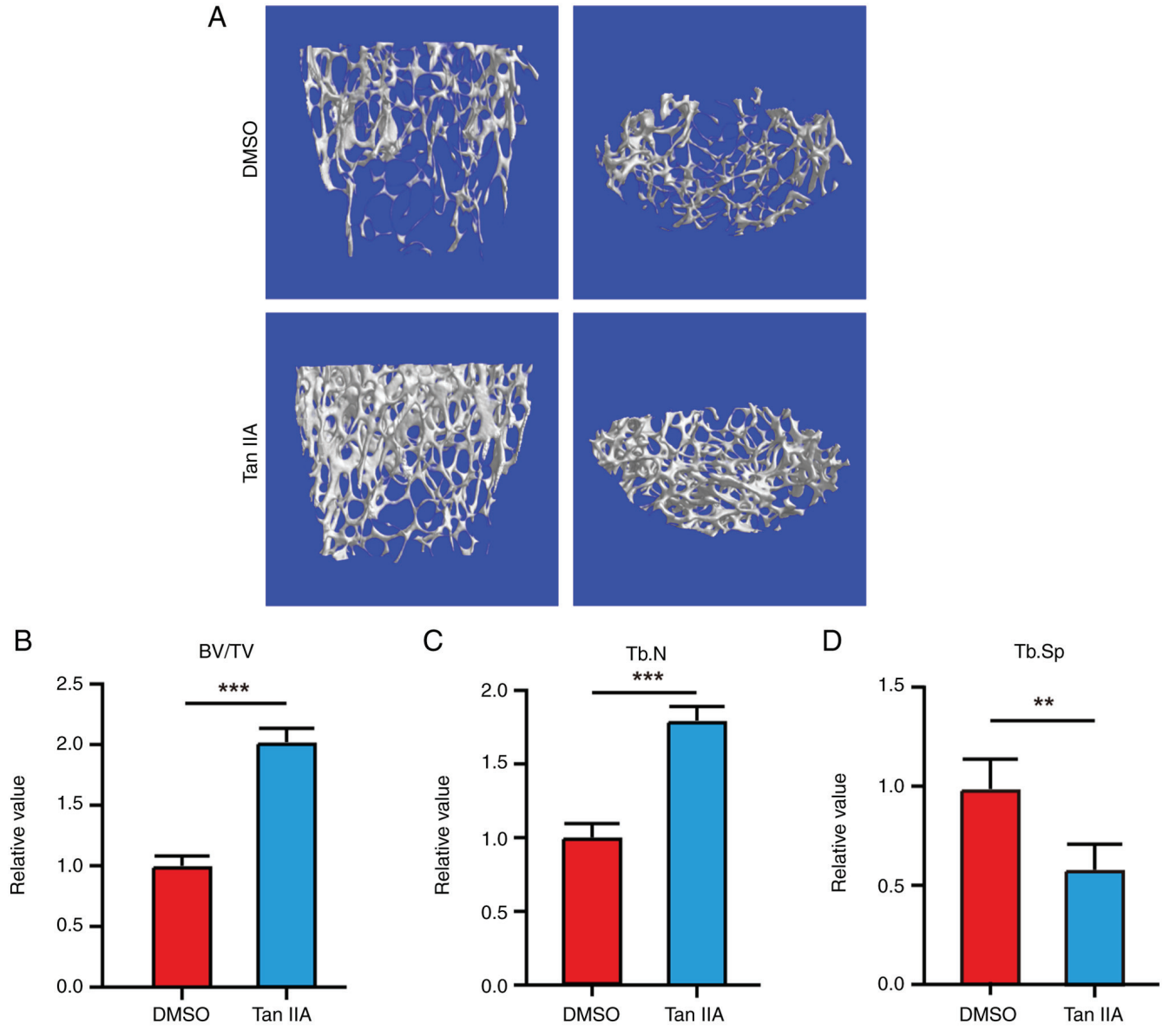

Figure 8. Tan IIA promotes BMSCs osteogenesis *in vivo*. (A) Micro-CT images of femur. Relative values of (B) BV/TV, (C) Tb. N and (D) Tb.Sp in Micro-CT analysis. **P<0.01, ***P<0.001. Tan IIA, Tanshinone IIA; BMSCs, bone marrow mesenchymal stem cells; CT, computed tomography; BV/TV, percent bone volume; Tb. N, trabecular number; Tb.Sp, trabecular separation.

with the CREB to promote osteogenic differentiation of MSCs by upregulating cyclin D1 and cyclin E1. In the current study, activation of AKT/CREB signaling following Tan IIA treatment was indicated by RNA-seq and it was further verified that Tan IIA promoted osteogenesis of BMSCs through the AKT/CREB signaling pathway. The present study also revealed the importance of activated TGFβ/Smad3 signaling by Tan IIA in inhibiting adipogenic differentiation of BMSCs. TGFβ plays crucial roles in a variety of biological processes through its downstream signaling molecules Smads (37). Smad3 is one of the most representative Smads and a number of researchers emphasize the central role of TGFβ/Smad3 signaling in suppressing adipogenesis (25-27). Downregulation of Smad3 by RNAi significantly increases the adipogenic differentiation of MSCs (25,27), while Smad3 knock out mice show smaller-size adipocytes when compared with wild-type mice (26). Thus, the present study provided a detailed mechanism of how Tan IIA promoted osteogenic differentiation and inhibited adipogenic differentiation ability of BMSCs.

The current study was not without limitations. First, although Tan IIA could promote osteogenic differentiation and inhibit adipogenic differentiation of BMSCs *in vitro*, these biological effects should be further verified in animal models with ANFH due to the more complex microenvironment *in vivo*. Furthermore, there was a lack of positive control drug in current study, so it was hard to determine to what extent Tan IIA has beneficial effects. Thus, the therapeutic potential of Tan IIA should be compared with a positive control drug in animal models with ANFH in further study.

In conclusion, Tan IIA could promote osteogenic differentiation potential of BMSCs by activating AKT signaling and suppress adipogenic differentiation potential of BMSCs by activating TGFβ signaling.

Acknowledgements

Not applicable.

Funding

The present study was supported by the Suzhou Science and Technology Development Plan (Medical and Health Science and Technology Innovation) Project (grant no. SKYD2022065).

Availability of data and materials

The RNA-seq data generated in the present study may be found in the NCBI under accession number PRJNA1131477 or at the following URL: https://www.ncbi.nlm.nih.gov/bioproject/PRJNA1131477. The other data generated in the present study may be requested from the corresponding author.

Authors' contributions

WW, HW, SFa and SFe designed the present study, collected the experimental data and wrote the original draft of the manuscript. WW, YF and XH conducted the image analysis, statistical analysis and wrote the original draft of the manuscript. HX and XS designed the present study and reviewed and edited the manuscript. YF and SFa administrated the project and edited the manuscript. WW and SFa confirm the authenticity of all the raw data. All authors read and approved the final version of the manuscript.

Ethics approval and consent to participate

The animal experiments were approved by the current the animal ethics committee of Suzhou Wujiang District Second People's Hospital (approval no. WZY2022056). The present study was conducted in accordance with ARRIVE guidelines.

Patient consent for publication

Not applicable.

Competing interests

The authors declare that they have no competing interests.

References

1. Konarski W, Poboży T, Śliwczyński A, Kotela I, Krakowiak J, Hordowicz M and Kotela A: Avascular necrosis of femoral head-overview and current state of the art. Int J Environ Res Public Health 19: 7348, 2022.
2. Rajpura A, Wright AC and Board TN: Medical management of osteonecrosis of the hip: A review. Hip Int 21: 385-392, 2011.
3. Sai Krishna MLV, Kar S, Kumar R, Singh H, Mittal R and Digge VK: The role of conservative management in the avascular necrosis of the femoral head: A review of systematic reviews. Indian J Orthop 57: 410-420, 2023.
4. Li Z, Wang W, Xu H, Ning Y, Fang W, Liao W, Zou J, Yang Y and Shao N: Effects of altered CXCL12/CXCR4 axis on BMP2/Smad/Runx2/Osterix axis and osteogenic gene expressions during osteogenic differentiation of MSCs. Am J Transl Res 9: 1680-1693, 2017.
5. Shapiro F, Connolly S, Zurakowski D, Menezes N, Olear E, Jimenez M, Flynn E and Jaramillo D: Femoral head deformation and repair following induction of ischemic necrosis: A histologic and magnetic resonance imaging study in the piglet. J Bone Joint Surg Am 91: 2903-2914, 2009.
6. Xu N, Liu H, Qu F, Fan J, Mao K, Yin Y, Liu J, Geng Z and Wang Y: Hypoxia inhibits the differentiation of mesenchymal stem cells into osteoblasts by activation of Notch signaling. Exp Mol Pathol 94: 33-39, 2013.
7. Benjamin S, Sheyn D, Ben-David S, Oh A, Kallai I, Li N, Gazit D and Gazit Z: Oxygenated environment enhances both stem cell survival and osteogenic differentiation. Tissue Eng Part A 19: 748-758, 2013.
8. Liu K, Ge H, Liu C, Jiang Y, Yu Y and Zhou Z: Notch-RBPJ pathway for the differentiation of bone marrow mesenchymal stem cells in femoral head necrosis. Int J Mol Sci 24: 6295, 2023.
9. Wei B, Sun C, Wan H, Shou Q, Han B, Sheng M, Li L and Kai G: Bioactive components and molecular mechanisms of *Salvia miltiorrhiza* Bunge in promoting blood circulation to remove blood stasis. J Ethnopharmacol 317: 116697, 2023.
10. Sun K, Xue Y, Zhang X, Li X, Zhao J, Xu X, Zhang X and Yang F: Tanshinone I alleviates steroid-induced osteonecrosis of femoral heads and promotes angiogenesis: In vivo and in vitro studies. J Orthop Surg Res 18: 474, 2023.
11. Wu Y, Zhang C, Wu J, Han Y and Wu C: Angiogenesis and bone regeneration by mesenchymal stem cell transplantation with danshen in a rabbit model of avascular necrotic femoral head. Exp Ther Med 18: 163-171, 2019.
12. Gao S, Liu Z, Li H, Little PJ, Liu P and Xu S: Cardiovascular actions and therapeutic potential of tanshinone IIA. Atherosclerosis 220: 3-10, 2012.
13. Xie J, Wang H, Song T, Wang Z, Li F, Ma J, Chen J, Nan Y, Yi H and Wang W: Tanshinone IIA and astragaloside IV promote the migration of mesenchymal stem cells by up-regulation of CXCR4. Protoplasma 250: 521-530, 2013.
14. Yuan P, Qin HY, Wei JY, Chen G and Li X: Proteomics reveals the potential mechanism of Tanshinone IIA in promoting the ex vivo expansion of human bone marrow mesenchymal stem cells. Regen Ther 21: 560-573, 2022.
15. Liu X, Niu Y, Xie W, Wei D and Du Q: Tanshinone IIA promotes osteogenic differentiation of human periodontal ligament stem cells via ERK1/2-dependent Runx2 induction. Am J Transl Res 11: 340-350, 2019.
16. Kim HJ and Kim SH: Tanshinone IIA enhances BMP-2-stimulated commitment of C2C12 cells into osteoblasts via p38 activation. Amino Acids 39: 1217-1226, 2010.
17. Abbuehl JP, Tatarova Z, Held W and Huelsken J: Long-term engraftment of primary bone marrow stromal cells repairs niche damage and improves hematopoietic stem cell transplantation. Cell Stem Cell 21: 241-255.e6, 2017.
18. Davaapil H, McNamara M, Granata A, Macrae RGC, Hirano M, Fitzek M, Aragon-Martin JA, Child A, Smith DM and Sinha S: A phenotypic screen of Marfan syndrome iPSC-derived vascular smooth muscle cells uncovers GSK3β as a new target. Stem Cell Rep 18: 555-569, 2023.
19. Chiang J and Martinez-Agosto JA: Effects of mTOR inhibitors on components of the salvador-warts-hippo pathway. Cells 1: 886-904, 2012.
20. Livak KJ and Schmittgen TD: Analysis of relative gene expression data using real-time quantitative PCR and the 2(-Delta Delta C(T)) method. Methods 25: 402-408, 2001.
21. Reggio A, Rosina M, Palma A, Cerquone Perpetuini A, Petrilli LL, Gargioli C, Fuoco C, Micarelli E, Giuliani G, Cerretani M, *et al*: Adipogenesis of skeletal muscle fibro/adipogenic progenitors is affected by the WNT5a/GSK3/β-catenin axis. Cell Death Differ 27: 2921-2941, 2020.
22. Li B and Dewey CN: RSEM: Accurate transcript quantification from RNA-Seq data with or without a reference genome. BMC Bioinformatics 12: 323, 2011.
23. Wang L, Feng Z, Wang X, Wang X and Zhang X: DEGseq: An R package for identifying differentially expressed genes from RNA-seq data. Bioinformatics 26: 136-138, 2010.
24. Xie C, Mao X, Huang J, Ding Y, Wu J, Dong S, Kong L, Gao G, Li CY and Wei L: KOBAS 2.0: A web server for annotation and identification of enriched pathways and diseases. Nucleic Acids Res 39 (Web Server Issue): W316-W322, 2011.
25. Guo W, Flanagan J, Jasuja R, Kirkland J, Jiang L and Bhasin S: The effects of myostatin on adipogenic differentiation of human bone marrow-derived mesenchymal stem cells are mediated through cross-communication between Smad3 and Wnt/beta-catenin signaling pathways. J Biol Chem 283: 9136-9145, 2008.

26. Tsurutani Y, Fujimoto M, Takemoto M, Irisuna H, Koshizaka M, Onishi S, Ishikawa T, Mezawa M, He P, Honjo S, *et al*: The roles of transforming growth factor-β and Smad3 signaling in adipocyte differentiation and obesity. Biochem Biophys Res Commun 407: 68-73, 2011.
27. Kim YJ, Hwang SJ, Bae YC and Jung JS: MiR-21 regulates adipogenic differentiation through the modulation of TGF-beta signaling in mesenchymal stem cells derived from human adipose tissue. Stem Cells 27: 3093-3102, 2009.
28. Cao H, Shi K, Long J, Liu Y, Li L, Ye T, Huang C, Lai Y, Bai X, Qin L and Wang X: PDGF-BB prevents destructive repair and promotes reparative osteogenesis of steroid-associated osteonecrosis of the femoral head in rabbits. Bone 167: 116645, 2023.
29. Kang H, Yang S and Lee J: Tauroursodeoxycholic acid enhances osteogenic differentiation through EGFR/p-Akt/CREB1 pathway in mesenchymal stem cells. Cells 12: 1463, 2023.
30. Gao B, Deng R, Chai Y, Chen H, Hu B, Wang X, Zhu S, Cao Y, Ni S, Wan M, *et al*: Macrophage-lineage TRAP+ cells recruit periosteum-derived cells for periosteal osteogenesis and regeneration. J Clin Invest 129: 2578-2594, 2019.
31. Baker N, Sohn J and Tuan RS: Promotion of human mesenchymal stem cell osteogenesis by PI3-kinase/Akt signaling, and the influence of caveolin-1/cholesterol homeostasis. Stem Cell Res Ther 6: 238, 2015.
32. Han J, Chai Y, Zhang XY, Chen F, Xu ZW, Feng Z, Yan Q, Wen SB and Wu YK: Gujiansan ameliorates avascular necrosis of the femoral head by regulating autophagy via the HIF-1α/BNIP3 pathway. Evid Based Complement Alternat Med 2021: 6683007, 2021.
33. Huang Z, Fu F, Ye H, Gao H, Tan B, Wang R, Lin N, Qin L and Chen W: Chinese herbal Huo-Gu formula for the treatment of steroid-associated osteonecrosis of femoral head: A 14-year follow-up of convalescent SARS patients. J Orthop Translat 23: 122-131, 2020.
34. Li ZR, Cheng LM, Wang KZ, Yang NP, Yang SH, He W, Wang YS, Wang ZM, Yang P, Liu XZ, *et al*: Herbal Fufang Xian Ling Gu Bao prevents corticosteroid-induced osteonecrosis of the femoral head-A first multicentre, randomised, double-blind, placebo-controlled clinical trial. J Orthop Translat 12: 36-44, 2017.
35. Li J, He C, Tong W, Zou Y, Li D, Zhang C and Xu W: Tanshinone IIA blocks dexamethasone-induced apoptosis in osteoblasts through inhibiting Nox4-derived ROS production. Int J Clin Exp Pathol 8: 13695-13706, 2015.
36. Du K and Montminy M: CREB is a regulatory target for the protein kinase Akt/PKB. J Biol Chem 273: 32377-32379, 1998.
37. Tzavlaki K and Moustakas A: TGF-β signaling. Biomolecules 10: 487, 2020.